Egypt. J. Chem. **Vol. 66**, No. 10 pp. 191 - 201 (2023)

Egyptian Journal of Chemistry

http://ejchem.journals.ekb.eg/

Influence of both Chemical Reaction and Electro-Osmosis on MHD Non-Newtonian Fluid Flow with Gold Nanoparticles

N. Hegazy [a], N. T. Eldabe [b], M. Y. Abou-zeid [b*], A.S. Abo Seliem [a] and A. A. Elenna [a]

[a]*Department of Mathematics, Faculty of Science, Kafrelsheikh University, Kafrelsheikh, Egypt*
[b]*Department of Mathematics, Faculty of Education, Ain Shams University, Cairo, Egypt*

Abstract

In this paper, the problem of electro-osmotic peristaltic motion of nano-coupled stress fluid with heat transfer through a non-uniform inclined channel is studied. The fluid obeys the power-law model and flows through a non-Darcy porous medium. Moreover, the effects of external magnetic field, thermal radiation, heat generation, Ohmic dissipation and chemical reaction are taken into consideration. The governing equations that describe the velocity, temperature and nanoparticles concentration are simplified under the assumption of long wavelength and low-Reynolds number. The resulting system of partial differential equations is solved numerically by using Rung-Kutta-Merson method. The solutions are obtained as functions of the physical problem parameters. The effects of these parameters on the obtained solutions are discussed and illustrated graphically through a set of figures. It is found that the axial velocity profiles decrease with the increase of electro-osmotic parameter.

Keywords: Non-Newtonian: nanofluid; Peristaltic flow; Non-Darcy porous medium; Electro-osmotic

1. Introduction

Nanofluids are a relatively new form of fluids in which (1–100 nm) nanoparticles are suspended in a base fluid. Nanoparticles that are often utilized include: metal carbides {SiC} or metals {Al, Cu} or oxides {Al_2O_3, CuO} or single / multi-walled nanotubes of carbon, etc. Whereas the most typically utilized base fluids include: water or ethylene glycols or polymer solutions, etc. Nanofluids have higher thermal conductivity when compared to base fluids. Therefore, nanofluids have attracted the regard of researchers owing to their considerable profits in industrial and biomedical areas such as vehicle cooling, solar water heating, domestic refrigerator, advanced nuclear systems, cancer therapeutics, and magnetic resonance imaging (MRI). Ardahaie et al. [1] investigated the effect of incorporating nanoparticles into blood flow in the presence of magnetic field in a porous blood artery. The creeping flow of a power-law nanofluid in a non-uniform inclined channel with peristalsis was studied by Abou-zeid and Mohamed [2]. Abou-zeid [3] investigated the effect of the Cattaneo-Christov heat flux on the MHD flow of a biviscosity nanofluid between two rotating disks via a porous medium. Khan et al. [4] studied the peristaltic flow of MHD nanofluids through an asymmetric channel. They utilized nanoparticles in three diverse shapes. It has been reported that nanoparticles with cylindrical shapes have much lower thermal efficiency than spherical and disc shapes. Eldabe et al. [5] studied the effects of Ohmic dissipation and mixed convection on the peristaltic flow of a non-Newtonian nanofluid between two co-axial tubes. Eldabe et al. [6] investigated the influence of the induced magnetic field on the flow of non-Newtonian nanofluid (Al_2O_3) through the boundary-layer containing gyrotactic microorganisms.

The physiological fluids of animals and humans are generally pumped by the ongoing episodic muscular oscillations of the tubes. These oscillations are believed to be induced by transverse contractions waves that propagate across the ducts walls. This sort of movement is known as peristalsis. It is renowned

*Corresponding author e-mail: mastermath2003@gmail.com; (M. Y. Abou-zeid).
EJCHEM use only: Received date 28 January 2023; revised date 05 February 2023; accepted date 05 February 2023
DOI: 10.21608/EJCHEM.2023.190175.7526

for carrying urine from the kidney to the bladder, chyme movement in the gastrointestinal tract, swallowing food through the esophagus, transferring eggs through the female fallopian tubes, and blood flow in small vessels of circulatory system, etc. It is also used in a variety of industrial and medical applications such as tube pumps, rollers, hose, open-heart surgery and heart-lung operation devices, and dialysis machines. An analytical study was done by Abou-zeid [7] to discuss the effects of couple stresses on MHD peristaltic motion of a non-Newtonian Jeffery nanofluid between co-axial tubes through a porous media. Eldabe et al. [8] investigated the peristaltic transport of a non-Newtonian power-law nanofluid inside a non-uniform inclined channel through a non-Darcy porous medium. Ibrahim and Abou-zeid [9] discussed the peristaltic flow of a Prandtl fluid with heat and mass transfer in a non-uniform channel with sinusoidal deformation. Devakar et al. [10] discussed the magnetic effects on the peristaltic motion of couple stress fluid in two concentric inclined tubes in which the inner tube is an endoscope and the outer tube has a sinusoidal wave traveling down its wall. The peristaltic motion of a Bingham plastic nanofluid through a vertical symmetric channel was studied by Abuiyada et al. [11]. Ismael et al. [12] studied the influences of entropy generation as well as slip velocity and temperature conditions on MHD micropolar biviscosity nanofluid flow through a porous medium in a channel with peristalsis. Ibrahim et al. [13] analyzed the problem of MHD mixed convection flow of Bingham nanofluid through a non-Darcy porous medium in a tube with peristalsis.

The term "electro-osmosis" refers to the movement of an electrolyte through a channel with a charged boundary as a result of an applied voltage. In recent decades, researchers have become interested in electro-osmosis due to its numerous uses in biological, industrial, and medical processes such as porous membranes, channel flow, fluid dialysis, botanical operations, human skin transport, and separation techniques. Tripathi et al. [14] presented a theoretical investigation of the peristaltic hydrodynamics of an aqueous electrolytic non-Newtonian Jeffrey biorheological fluid in the presence of an applied axial electric field through an asymmetric microchannel. Eldabe et al. [15] examined the influence of electro-osmosis on the peristaltic transport of an incompressible MHD nanofluid across a porous media. The simultaneous effects of the magnetic field, heat absorption, and mixed convection on the electroosmotically induced peristaltic transport of copper particles in the blood were discussed by Noreen et al. [16]. Tanveer et al. [17] examined the natural convective flow of MHD third-grade fluid caused by the peristaltic wave in a microchannel with electro-osmosis. The electroosmotic flow of MHD nanofluids through an asymmetric microfluidic channel was investigated by Noreen et al. [18]. The electroosmotic peristaltic pumping of MHD nanofluid in an asymmetric microfluidic channel with zeta potentials was studied by Noreen et al. [19]. Lu et al. [20] investigated heat transfer applications in curved micro-channel driven by electroosmosis and peristaltic pumping.

The current work is an extension to Eldabe et al. [8] to include the influences of electro-osmosis, couple stress, and chemical reaction on the peristaltic flow of a power-law nanofluid inside an inclined non-uniform channel. The system of non-linear partial differential equations that governs this phenomenon is complicated. It is simplified using the approximation of low Reynolds number and long-wavelength approximation. Then, this system of equations is solved numerically. The impacts of various parameters on the flow variables are illustrated by sketching graphs.

2. Mathematical description

Let us consider two-dimensional peristaltic transport of an incompressible non-Newtonian nanofluid obeying power-law model in a non-uniform channel with heat transfer. It is assumed that the electric field E_x is applied axially to the fluid flow and the magnetic field B_0 is applied transversely. The radius of the non-uniform sinusoidal channel (as modelled in Chaube et al. [21]) is described by the following equation:

$$h(x) = a + x\tan(\alpha) + b\sin(2\pi x/\lambda) \qquad (1)$$

where a, b, λ, x, α are half width of the opening of the channel, the amplitude of the wave, the wavelength, the axial displacement, the angle between the wall and the axis of symmetry of the channel, respectively.

Hayat et al. [22] define the relation between the stress tensor and the rate of strain in the power-law model as follows:

$$\boldsymbol{S} = \mu_0 |tr(\boldsymbol{A}_1)^2|^m \boldsymbol{A}_1 \qquad (2)$$

where $\boldsymbol{A}_1$ is the rate of deformation tensor, and μ_0 is the dynamic viscosity. Here, m is the power-law index. The fluid behaves like shear-thinning or Newtonian or shear-thickening according to whether $m<0$ or $m=0$ or $m>0$.

The transformations between the fixed frame (X,Y) and the wave frame (x,y) which moves with the speed c are represented as follows:

$$x = X - ct,\ y = Y, \tag{3}$$

$$u(x,y) = U(X,Y;t) - c, v(x,y) = V(X,Y,t) \tag{4}$$

The governing equations for an incompressible power-law nanofluid flow in the wave frame after applying Eqs. (3) and (4) are given as [8]:

Continuity equation

$$\frac{\partial u}{\partial x} + \frac{\partial v}{\partial y} = 0 \tag{5}$$

Equations of motion

$$\rho_f\left(u\frac{\partial u}{\partial x} + v\frac{\partial u}{\partial y}\right) = -\frac{\partial P}{\partial x} + \frac{\partial S_{xx}}{\partial x} + \frac{\partial S_{yx}}{\partial y} - \eta\left(\frac{\partial^4 u}{\partial x^4} + \frac{\partial^4 u}{\partial x^2 \partial y^2} + \frac{\partial^4 u}{\partial y^4}\right) - \frac{\mu_0}{k}u - \rho_f c_s u\sqrt{u^2+v^2} - \rho_f\, g\sin(\theta) - \sigma B_0{}^2 u + \rho_e E_x \tag{6}$$

$$\rho_f\left(u\frac{\partial v}{\partial x} + v\frac{\partial v}{\partial y}\right) = -\frac{\partial P}{\partial y} + \frac{\partial S_{yy}}{\partial x} + \frac{\partial S_{xy}}{\partial y} - \eta\left(\frac{\partial^4 v}{\partial x^4} + \frac{\partial^4 v}{\partial x^2 \partial y^2} + \frac{\partial^4 v}{\partial y^4}\right) - \frac{\mu_0}{k}v - \rho_f c_s v\sqrt{u^2+v^2} - \rho_f\, g\cos(\theta) \tag{7}$$

Energy equation

$$(\rho c)_f\left(u\frac{\partial T}{\partial x} + v\frac{\partial T}{\partial y}\right) = K\left(\frac{\partial^2 T}{\partial x^2} + \frac{\partial^2 T}{\partial y^2}\right) + (\rho c)_p\left[\begin{array}{l} D_B\left(\frac{\partial T}{\partial x}\frac{\partial f}{\partial x} + \frac{\partial T}{\partial y}\frac{\partial f}{\partial y}\right) + \\ \frac{D_T}{T_0}\left(\left(\frac{\partial T}{\partial x}\right)^2 + \left(\frac{\partial T}{\partial y}\right)^2\right)\end{array}\right] + S_{xx}\frac{\partial u}{\partial x} + S_{yx}\frac{\partial u}{\partial y} + S_{xy}\frac{\partial v}{\partial x} + S_{yy}\frac{\partial v}{\partial y} + Q_0(T - T_1) + \sigma B_0{}^2 u^2 - \frac{\partial q_r}{\partial y} + \eta\left[\begin{array}{l}\left(\frac{\partial^2 u}{\partial x^2} + \frac{\partial^2 u}{\partial y^2}\right)^2 + \\ \left(\frac{\partial^2 v}{\partial x^2} + \frac{\partial^2 v}{\partial y^2}\right)^2\end{array}\right] \tag{8}$$

Nanoparticles concentration equation

$$u\frac{\partial f}{\partial x} + v\frac{\partial f}{\partial y} = D_B\left(\frac{\partial^2 f}{\partial x^2} + \frac{\partial^2 f}{\partial y^2}\right) + \frac{D_T}{T_0}\left(\frac{\partial^2 T}{\partial x^2} + \frac{\partial^2 T}{\partial y^2}\right) - A(f - f_1) \tag{9}$$

in which u is the axial velocity, v is the transverse velocity, y is the transverse coordinate, ρ_f is the density of the fluid, P is the fluid pressure, S_{ij} are the stress tensor components of power-law model, η is the couple stress coefficient, μ_0 is the dynamic viscosity of the fluid, k is the permeability constant of the porous medium, c_s is Forchheimer constant, g is the gravitational acceleration, θ is the inclination angle of the channel, σ is the fluid electrical conductivity, ρ_e is the electric charge number density, $(\rho c)_f$ is the heat capacity of the fluid, T is the fluid temperature, K is the thermal conductivity, D_B is the Brownian motion coefficient, f is the nanoparticles concentration, D_T is the thermophoretic diffusion coefficient, T_0 is the fluid temperature at $y = 0$, Q_0 is the volumetric rate of heat generation, T_1 is the fluid temperature at $y = h$, q_r is the radiation heat flux, A is the chemical reaction parameter, f_1 is the nanoparticles concentration at $y = h$.

Using Rosseland approximation for radiation in Eldabe et al. [8], the radiation heat flux is given by:

$$q_r = -\frac{4\sigma^*}{3k_R}\frac{\partial T^4}{\partial y} \tag{10}$$

the temperature variationd within the fluid are supposed to be very small, therefore T^4 can be expressed in Taylor series about T_1 and the higher-order terms are ignored. Hence, T^4 may be expressed as a linear function of temperature which is given by

$$T^4 \approx 4T_1{}^3 T - 3T_1{}^4 \tag{11}$$

According to Prakash and Tripathi [23], Poisson equation is utilized to characterize electronic potential ϕ generated across the electrical double layer (EDL):

$$\nabla^2\phi = -\frac{\rho_e}{\varepsilon_0} \tag{12}$$

where ρ_e denotes the total charge density and ε_0 the dielectric permittivity.

From the Gaussian law, it is found that:

$$\boldsymbol{E} = -\nabla \phi \tag{13}$$

The net charge density ρ_e follows the Boltzmann distribution is given as Eldabe et al. [15]:

$$\rho_e = ze\,(n^+ - n^-) \tag{14}$$

where e specifies electric charge, n^+ and n^- are anions and cations having bulk concentration n_0 and z the charge balance of species.

Applying the Nernst-Planck equation given by Tripathi et al. [24], the distribution of ions within the fluid is described as:

$$u\frac{\partial n^{\pm}}{\partial x} + v\frac{\partial n^{\pm}}{\partial y} = D\left(\frac{\partial^2 n^{\pm}}{\partial x^2} + \frac{\partial^2 n^{\pm}}{\partial y^2}\right) + \frac{Dze}{k_B \hat{T}}\left[\frac{\partial}{\partial x}\left(n^{\pm}\frac{\partial \phi}{\partial x}\right)\right] + \frac{\partial}{\partial y}\left(n^{\pm}\frac{\partial \phi}{\partial y}\right) \tag{15}$$

in the above equation, D is the ionic diffusivity, $\hat{T}$ defines the mean temperature of the ionic solution and k_B is Boltzmann constant.

It is now convenient to introduce the dimensionless quantities listed below.

$$\left\{\begin{array}{l}
\bar{x} = \frac{x}{\lambda},\ \bar{y} = \frac{y}{a},\ \bar{u} = \frac{u}{c},\ \bar{v} = \frac{v}{c\delta},\ \bar{h} = \frac{h}{a},\ \varphi = \frac{b}{a},\ \bar{n} = \frac{n}{n_0},\\
\bar{P} = \frac{a^2}{\lambda c \mu_0}\left(\frac{a^2}{2c^2}\right)^m P,\ \bar{S} = \frac{a}{c\mu_0}\left(\frac{a^2}{2c^2}\right)^m S,\ \bar{U}_{HS} = -\frac{\varepsilon_0 k_B \hat{T} E_x}{ezc\mu_0},\\
\bar{\phi} = \frac{a^2 ez}{k_B \hat{T}}\left(\frac{a^2}{2c^2}\right)^m,\ \delta = \frac{a}{\lambda},\ R_e = \frac{\rho_f c a}{\mu_0}\left(\frac{a^2}{2c^2}\right)^m,\ F_r = \frac{\rho_f c_s a^2 c_f}{\mu_0 \sqrt{k}},\\
M = \frac{\sigma B_0^2 a}{\rho_f c},\ F = \frac{c\mu_0}{\rho_f g a^2}\left(\frac{2c^2}{a^2}\right)^m,\ D_a = \frac{\rho_f c k}{a\mu_0},\ \alpha^2 = \frac{a^2\mu_0}{\eta}\left(\frac{2c^2}{a^2}\right)^m,\\
m_e = \sqrt{\frac{2n_0 e^2 z^2 a^2}{\varepsilon_0 k_B \hat{T}}},\ Pr = \frac{(\rho c)_f c a}{k_c},\ E_c = \frac{c^2}{c_f (T_0 - T_1)},\\
Q = \frac{Q_0 a}{(\rho c)_f c},\ R = \frac{4\sigma^* T_1^3}{k_c k_R},\ N_b = \frac{(\rho c) p D_B (f_0 - f_1)}{(\rho c)_f c a},\\
N_t = \frac{(\rho c) p D_T (T_0 - T_1)}{T_0 (\rho c)_f c a},\\
Sc = \frac{c a}{D_B},\ \gamma = \frac{Aa}{c},\ \beta = \frac{L}{a}
\end{array}\right. \tag{16}$$

Using the aforementioned non-dimensional quantities in Eqs. (5)–(9) and Eqs. (12)–(15), after dropping the bars, and taking into consideration low Reynolds number and long wavelength ($\delta \approx 0$), the resultant equations are as follows:

$$\frac{\partial P}{\partial x} = \frac{\partial S_{xy}}{\partial y} - \frac{1}{\alpha^2}\frac{\partial^4 u}{\partial y^4} - R_e\left(M + \frac{1}{D_a}\right)(u+1) - R_e F_s (u+1)^2 - \frac{\sin(\theta)}{F} + m_e^{\,2} U_{HS}\phi \tag{17}$$

$$\frac{\partial P}{\partial y} = 0 \tag{18}$$

$$\frac{1}{Pr}\left(1 + \frac{4}{3}\right)\frac{\partial^2 T}{\partial y^2} + N_b \frac{\partial T}{\partial y}\frac{\partial f}{\partial y} + N_t\left(\frac{\partial T}{\partial y}\right)^2 + \frac{E_c}{R_e} S_{yx}\frac{\partial u}{\partial y} + Q\,T + M\,E_c\,(u+1)^2 + \frac{E_c}{\alpha^2 R_e}\left(\frac{\partial^2 u}{\partial y^2}\right)^2 = 0 \tag{19}$$

$$\frac{\partial^2 f}{\partial y^2} + \frac{N_t}{N_b}\frac{\partial^2 T}{\partial y^2} - \gamma S_c\, f = 0 \tag{20}$$

$$\frac{\partial^2 \phi}{\partial y^2} = m_e^{\,2}\left(\frac{n^- - n^+}{2}\right) \tag{21}$$

$$\frac{\partial^2 n^{\pm}}{\partial y^2} \pm \frac{\partial}{\partial y}\left(n^{\pm}\frac{\partial \phi}{\partial y}\right) = 0 \tag{22}$$

where $S_{xy} = S_{yx} = \left(\frac{\partial u}{\partial y}\right)^{2m+1}$ 、 (23)

Equation (22) is solved subjected to $n_{\pm} = 1$ at $\phi = 0$ and $\frac{\partial n_{\pm}}{\partial y} = 0$ at $\frac{\partial \phi}{\partial y} = 0$ (bulk conditions). Therefore, the resulting solution is expressed as:

$$n_{\pm} = e^{\mp\phi} \tag{24}$$

By combining Eqs. (21) and (24), we obtain the Poisson-Boltzmann paradigm:

$$\frac{\partial^2 \phi}{\partial y^2} = m_e^{\,2}\,sinh(\phi) \tag{25}$$

Under Debye-Hückel's linearization, $sinh(\phi) \approx \phi$, hence,

$$\frac{\partial^2 \phi}{\partial y^2} = m_e^{\,2}\,\phi \tag{26}$$

Direct integration of equation (25) is performed subjected to the boundary conditions $\phi = 1$ at $y = h$ and $\frac{\partial \phi}{\partial y} = 0$ at $y = 0$. The resulting electric potential function is given as:

$$\phi = \frac{cosh(m_e\, y)}{cosh(m_e\, h)} \tag{27}$$

The adherence dimensionless boundary conditions are:

$$\frac{\partial u}{\partial y} = 0,\ \frac{\partial^2 u}{\partial y^2} = 0,\ T = 1,\ f = 1$$
$$at\ \ y = 0$$
$$u = -1 - \beta \frac{\partial u}{\partial y},\ \frac{\partial^2 u}{\partial y^2} = 0,\ T = 0,\ f = 0$$
$$at\ \ y = h = 1 + \frac{x}{\delta}\tan(\theta) + \varphi \sin(2\pi x) \tag{28}$$

3. Method of solution

To solve the above system of equations (17)-(20) with the boundary conditions (28), the subroutine D02HAF in NAG Fortran library is used. The shooting technique is then applied. This subroutine is essential to guess the starting values of initial and terminal conditions that are missing. The Rung-Kutta-Merson technique of order five is used to solve the governing equations (17)-(20). In this subroutine, we employ variable step size in order to manage the local truncation error. The modified Newton-Raphson technique is then used to obtain successive corrections for the predicted boundary values. The process is continued repeatedly until convergence is achieved, i.e., until the absolute values of the difference between every two successive approximations of the missing conditions is less than ε (in our problem ε is taken = 10-8).

Let $u = Y_1$, $T = Y_6$, $f = Y_8$.

Hence, Eqs. (17), (18), (19), (20) and (28) can be written as follows:

$$Y_1' = Y_2, Y_2' = Y_3, Y_3' = Y_4, Y_4' = Y_5;$$
$$Y_5 = \alpha^2 \begin{bmatrix} (2m+1)\,Sign(Y_2)(Y_2)^{2m} - \frac{\partial P}{\partial x} - R_e(M + \frac{1}{D_a})(Y_1 + 1) \\ - R_e F_r (Y_1 + 1)^2 - \frac{\sin(\theta)}{F} + m_e{}^2 U_{HS}\phi \end{bmatrix} \tag{29}$$

$$Y_6' = Y_7;$$
$$Y_7' = \left(\frac{-3Pr}{3+4}\right) \begin{bmatrix} N_b Y_7 Y_9 + N_t (Y_7)^2 + \frac{E_c}{R_e}(Y_2)^{2m+2} + \\ Q\, Y_6 + M\, E_c (Y_1 + 1)^2 + \frac{E_c}{\alpha^2 R_e}(Y_3)^2 \end{bmatrix} \tag{30}$$

$$Y_8' = Y_9;\ Y_9' = -\frac{N_t}{N_b} Y_7 + \gamma S_c Y_8 \tag{31}$$

$$Y_2 = 0, Y_3 = 0, Y_6 = Y_8 = 1\ at\ y = 0$$
$$Y_1 = -1 - \beta Y_2\ , Y_3 = Y_6 = Y_8 = 0\ at\ y = h \tag{32}$$

4. Results and discussion

In order to investigate the physical significance of the problem, we derived the numerical solutions of the axial velocity, temperature and nanoparticles concentration. The effects of various parameters entering the problem are discussed through the figures (1)-(9). These figures are depicted for a system whose particulars are following dimensionless numbers:

$$m = 0.5,\ \alpha = 0.5,\ R_e = 1,\ M = 2,$$
$$D_a = 0.5,\ F_r = 1.5,\ F = 2,\ m_e = 0.1,$$
$$U_{HS} = 0.5,\ Pr = 1,\ R = 4,\ N_b = 0.5,$$
$$N_t = 1.5,\ E_c = 1,\ Q = 2,\ \gamma = 0.5,$$
$$S_c = 0.5,\ \frac{\partial P}{\partial x} = -3,\ \theta = \pi/4,\ \beta = 2.$$

Figures (1) and (2) appear the conduct of the axial velocity u with the transverse coordinate y for various values of the pressure gradient $\frac{\partial P}{\partial x}$ and electro-osmotic parameter m_e, respectively. It is clear from Fig. (1) that the velocity profiles *u* decreases with the

raising of electro-osmotic parameter m_e. The reason behind this trend is EDL (electric double layer). It means flow of fluid resists in the presence of EDL. It is found that the raising of the magnetic parameter M has the same effect on the velocity profile as electro-osmotic parameter m_e. This is due to the magnetic field acts in the transverse direction of the transport phenomena. Sincethe difference of the magnetic parameter Mcauses the differenceof the Lorentz forces. The Lorentz force is a drag-like force that creates more resistance to transport phenomena and reduces the fluid velocity. The figure is omitted here to save space and avoid repetition. It is shown from Fig. (2) that an increase in the pressure gradient $\frac{\partial P}{\partial x}$ causes an increase in the velocity profile u. In general, such result could be applicable potential in improving fluid flow in the biological, physical and engineering processes. Also, Figures (3) and (4) show the effect of increasing the inclination angel of the channel θ and the slip parameter β on the axial velocity u. It is clear from these figures that the effects of θ and β on u is similar to the effect of pressure gradient $\frac{\partial P}{\partial x}$ on u.

The temperature distribution T with the transverse coordinate y for various values of the Reynolds number Re and Eckert number E_c, illustrate in Figures (5) and (6), respectively. The results which obtained in Fig. (5) are in agreement with Eldabe et al. [25], Abou-zeid [26]. It could be analyzed from Fig. (5) that the large value of Eckert number E_c enhances the temperature profile T. Physically, heat dissipation is characterized by Eckert number E_c. In viscous fluid, the increase of the kinetic energy produces internal heat energy (this is what we call viscous dissipation) which in terms enhances the fluid temperature.It is evident from Fig. (6) that the temperature profile T decreases as the Reynolds numberR_e increases. It is worth to indicate that the Reynolds number is the proportion of the inertia forces to the viscous forces in the fluid. Therefore, the viscous force decreases as the Reynolds number increases and as a result of that, the temperature profile decreases. Furthermore, the significance of the Reynolds number is that it helps predict flow patterns in various fluid flow situations. At low Reynolds numbers, flows tend to be dominated by laminar flow, while at high Reynolds numbers of flows tend to be turbulent.

Figures (7) through (9) show the change of the nanoparticles concentration f against the transverse coordinate y for various values of the thermal radiation parameter R, thermophoresis parameter N_t and the power-law index$m$, respectively. The nanoparticles concentration f increases with increasing the thermal as shown in fig (7). Physically, increasing the diameter of nanoparticles indicates that the concentration of the fluid increases. This can be employed as factors for radiation oncology where they may be utilized to deliver therapeutic agents, create a localized increase in radiation dosages, and target tumor cells selectively for localized damage. Fig. (8) shows that the nanoparticles concentration f increases as the power-law index$m$ increases. The nanoparticle concentration f is seen to decrease as the thermophoresis parameter N_t increases in Fig. (9). As in thermophoresis, particles are moved away from hot region to cold region. This leads to disturbance of nanoparticles and high values of the thermophoresis parameter result in increasing nanoparticles convection because of large random disturbance. Thus, the concentration of nanoparticles decreases. The result which is obtained in Fig. (9) is in agreement with Abou-zeid and Mohamed [27].

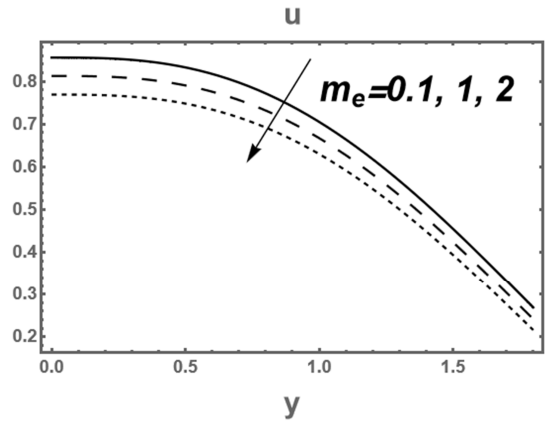

Fig. (1) The axial velocity is plotted against *y* for various values of m_e.

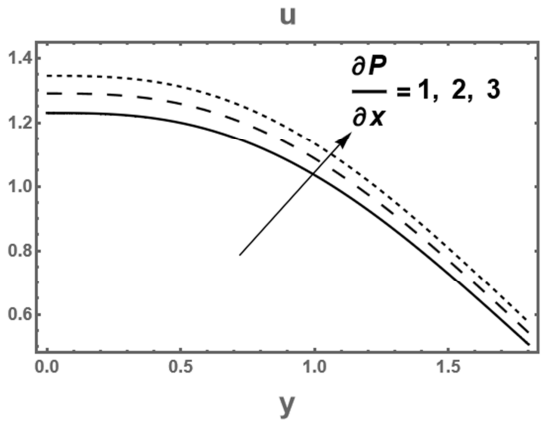

Fig. (2) The axial velocity is plotted against *y* for various values of $\frac{\partial P}{\partial x}$.

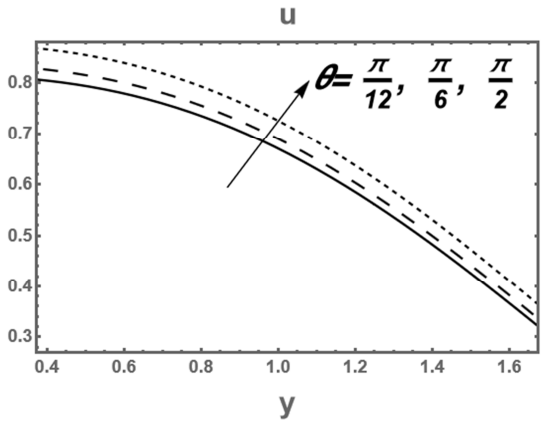

Fig. (3) The axial velocity is plotted against *y* for various values of θ.

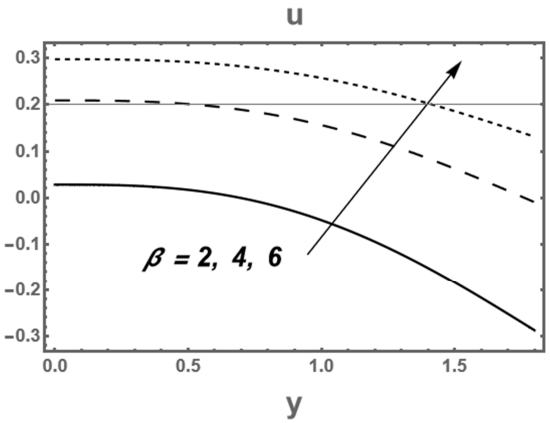

Fig. (4) The axial velocity is plotted versus *y* for various values of β.

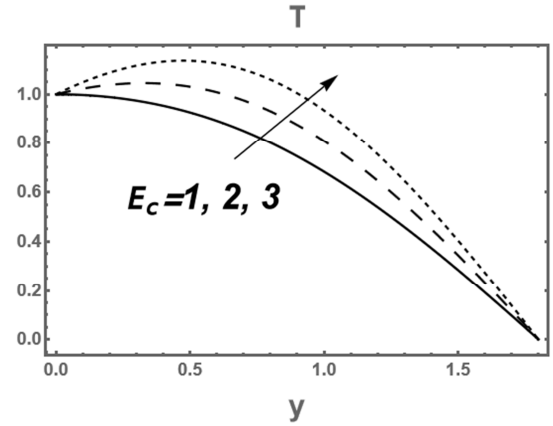

Fig. (5) The temperature is plotted against *y* for various values of E_c.

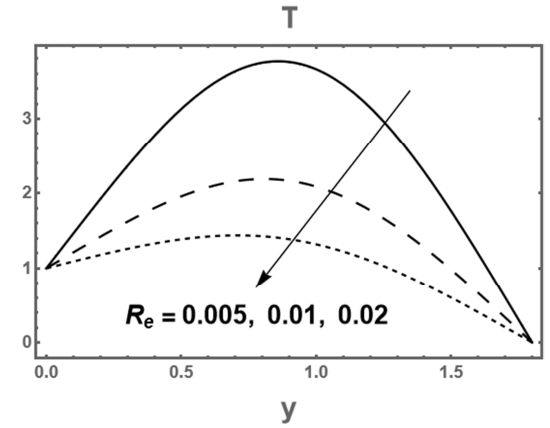

Fig. (6) The temperature is plotted against *y* for various values of R_e.

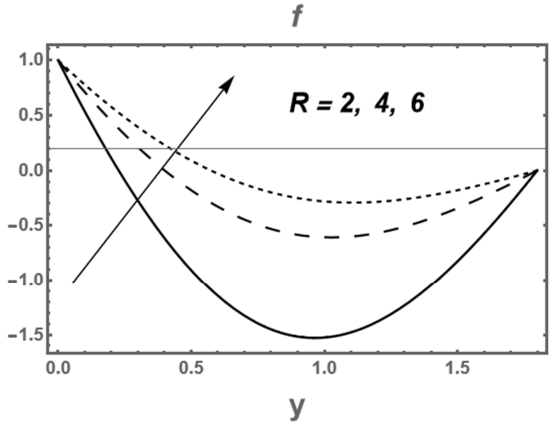

Fig. (7) The nanoparticles concentration is plotted against *y* for various values of *R*.

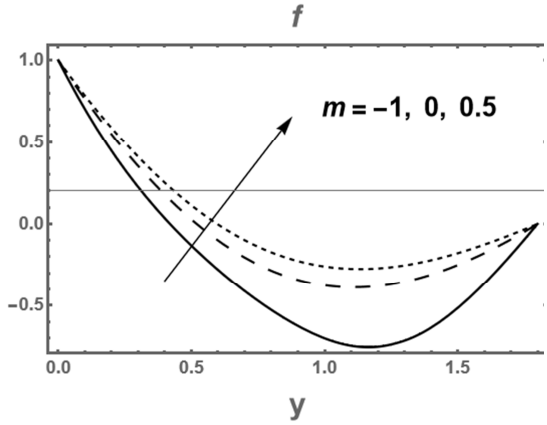

Fig. (8) The nanoparticles concentration is plotted against *y* for various values of *m*.

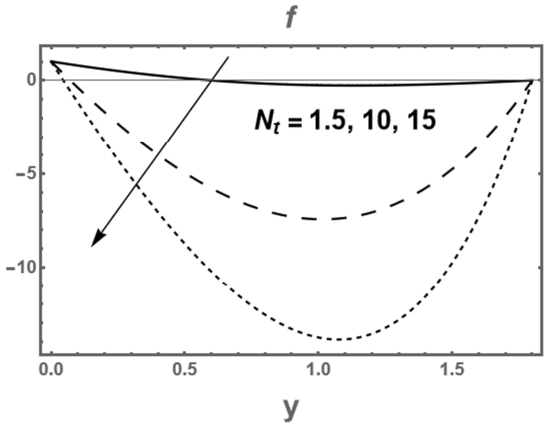

Fig. (9) The nanoparticles concentration is plotted against *y* for various values of N_t.

5. Conclusions

The objective of this study is to focus on the influence of coupled-stress, thermal radiation, Ohmic dissipation and chemical reaction on power-law nanofluid in a non-uniform inclined channel. Variable surface temperature and convective boundary conditions for both temperature and nanofluid concentration are also considered. Long wavelength and low Reynolds number are utilized to simplify our system from non-linear partial differential equations to ordinary differential equations in order to make it easy to solve. Then, numerical solutions for the axial velocity, temperature, and nanoparticles concentration distributions are obtained using the Rung-Kutta-Merson method. The effects of the various physical embedded parameters on these distributions are discussed numerically as well as graphically and represented via a set of graphs. Physically, our problem corresponds to the behavior of motion through most of the physiological organs like small blood vessels, ducts afferents of the male reproductive tracts, esophagus, lymphatic vessels, and the cervical canal [28-54]. The main outcomes of the present investigation are summarized as follows:

1) The axial velocity distribution *u*increases as the parameters *Da*, *Pr*, *Q* and $\frac{\partial P}{\partial x}$ increase, whereas it decreases as the parameters α, *Re*, $F_r$and M increase.
2) The relation between the velocity *u* and the normal axis *y* seems to be a parabola with an upper vortex for various values of these parameters.
3) An increase of Eckert number E_c and a decrease of Reynolds numberR_e cause an increment of the temperature distribution *T*.

4) By increasing the normal axis y, the temperature T for various values of problem physical parameters becomes greater and ends up with the maximum value at the right wall of the channel.
5) As the thermal radiation parameter R increase, the nanoparticles concentration increases, however, as the thermophoresis parameter N_t increase, the nanoparticles concentration decrease.
6) When compared to temperature behavior, the concentration of nanoparticles behaves in the opposite way.

6. References

[1] Ardahaie, S. S., Amiri, A. J., Amouei, A., Hosseinzadeh, Kh. & Ganji, D. D., Investigating the effect of adding nanoparticles to the blood flow in presence of magnetic field in a porous blood arterial. *Inform. Med. Unlocked* **10**, 71–81 (2018).

[2] Abou-zeid, M. Y. & Mohamed, M. A., Homotopy perturbation method to creeping flow of non-Newtonian power-law nanofluid in a non-uniform inclined channel with peristalsis. *Z. Naturforsch. A.***72**(10), 899–907 (2017).

[3] Abou-zeid, M. Y., Implicit homotopy perturbation method for MHD non-Newtonian nanofluid flow with Cattaneo-Christov heat flux due to parallel rotating disks. *J. Nanofluids***8**(8), 1648–1653 (2019).

[4] Khan, L. A., Raza, M., Mir, N. A. & Ellahi, R., Effects of various shapes of nanoparticles on peristaltic flow of MHD nanofluids filled in an asymmetric channel. *J. Therm. Anal. Calorim.***140**(3), 879–890 (2020).

[5] Eldabe, N. T., Abou-zeid, M. Y., Abosaliem, A., Elana A. & Hegazy, N., Homotopy perturbation approach for Ohmic dissipation and mixed convection effects on non-Newtonian nanofluid flow between two co-axial tubes with peristalsis. *Int. J. Appl. Electromagn. Mech.***67**(2), 153–163 (2021).

[6] Eldabe, N. T., Rizkallah, R. R., Abou-zeid, M. Y. & Ayad, V. M., Effect of induced magnetic field on non-Newtonian nanofluid Al_2O_3 motion through boundary-layer with gyrotactic microorganisms. *Therm. Sci.***26**(1B), 411–422 (2022).

[7] Abou-zeid, M. Y., Homotopy perturbation method for couple stresses effect on MHD peristaltic flow of a non-Newtonian nanofluid. *Microsyst. Technol.***24**(12), 4839–4846 (2018).

[8] El-Dabe, N. T., Abou-zeid, M. Y., Mohamed, M. A. & Abd-Elmoneim, M. M., MHD peristaltic flow of non-Newtonian power-law nanofluid through a non-Darcy porous medium inside a non-uniform inclined channel. *Arch. Appl. Mech.***91**(3), 1067–1077 (2021).

[9] Ibrahim, M.G. & Abou-zeid, M.Y. Influence of variable velocity slip condition and activation energy on MHD peristaltic flow of Prandtl nanofluid through a non-uniform channel. *Sci Rep* **12**, 18747 (2022).

[10] Devakar, M., Ramesh, K. & Vajravelu, K., Magnetohydrodynamic effects on the peristaltic flow of couple stress fluid in an inclined tube with endoscope. *J. Comput. Math. Data Sci.***2**, 100025 (2022).

[11] Abuiyada, A. J., Eldabe, N. T., Abou-zeid, M. Y., & El Shaboury, S. M., Effects of Thermal Diffusion and Diffusion Thermo on a Chemically Reacting MHD Peristaltic Transport of Bingham Plastic Nanofluid. *J. Adv. Res. Fluid Mech. Therm. Sci.***98**(2), 24–43 (2022).

[12] Ismael, A., Eldabe, N. T., Abou-zeid, M. Y. & El Shaboury, S. M., Entropy generation and nanoparticles Cu O effects on MHD peristaltic transport of micropolar non-Newtonian fluid with velocity and temperature slip conditions. *Egypt. J. Chem.***65**(9), 715–722 (2022).

[13] Ibrahim, M. G., Abdallah, N. F. & Abou-zeid, M. Y., Activation energy and chemical reaction effects on MHD Bingham nanofluid flow through a non-Darcy porous media. *Egypt. J. Chem*. **65**(13), 137-144 (2022).

[14] Tripathi, D., Jhorar, R., Bég, O. A. &Shaw, S., Electroosmosis modulated peristaltic biorheological flow through an asymmetric microchannel: mathematical model. *Meccanica***53**(8), 2079–2090 (2018).

[15] El-dabe, N. T., Moatimid, G. M., Hassan, M. A. & Godh, W. A., Electro-osmotic and Hall current effects on the nanofluid flow through porous medium with wall properties. *Int. J. Appl. Eng. Res.***14**(16), 3552–3565 (2019).

[16] Noreen, S., Waheed, S. & Lu, D. C., Electrothermal transport via copper nanoparticles in a microchannel propagated by peristalsis. *SN Appl. Sci.***2**(9), 1559 (2020).

[17] Tanveer, A., Mahmood, S., Hayat, T. & Alsaedi,

A., On electroosmosis in peristaltic activity of MHD non-Newtonian fluid. *Alex. Eng. J.***60**(3), 3369–3377 (2021).

[18] Noreen, S., Waheed, S., Lu, D. C. &Hussanan, A., Entropy generation in electromagnetohydrodynamic water based three Nano fluids via porous asymmetric microchannel. *Eur. J. Mech. B Fluids***85**, 458-466 (2021).

[19] Noreen, S., Waheed, S. & Hussanan, A., Peristaltic motion of MHD nanofluid in an asymmetric micro-channel with Joule heating, wall flexibility and various zeta potential. *Bound. Value Probl.***2019**, 12 (2019).

[20] Lu, D. C., Noreen, S., Waheed, S. & Tripathi, D., Heat transfer applications in curved micro-channel driven by electroosmosis and peristaltic pumping. *J. Mech. Med. Biol.* **22**(05), 2250030 (2022).

[21] Chaube, M. K., Tripathi, D., Bég, O. A., Sharma, S. & Pandey, V. S., Peristaltic creeping flow of power law physiological fluids through a non uniform channel with slip effect. *Appl. Bionics Biomech.***2015**, 152802 (2015).

[22] Hayat, T., Yasmin, H. & Alsaedi, A., Convective heat transfer analysis for peristaltic flow of power-law fluid in a channel. *J. Braz. Soc. Mech. Sci. Eng.***37**(2), 463–477 (2015).

[23] Prakash, J. & Tripathi, D., Electroosmotic flow of Williamson ionic nanoliquids in a tapered microfluidic channel in presence of thermal radiation and peristalsis. *J. Mol. Liq.***256**, 352–371 (2018).

[24] Tripathi, D., Bhushan, S. & Bég, O. A., Analytical study of electro-osmosis modulated capillary peristaltic hemodynamics. *J. Mech. Med. Biol.* **17**(3), 1750052 (2017).

[25] Eldabe, N. T., Abou-zeid M.Y. & Younis, Y. M., Magnetohydrodynamic peristaltic flow of Jeffry nanofluidwith heat transfer through a porous medium in a vertical tube. *Appl. Math. Inf. Sci.***11**(4), 1097–1103 (2017).

[26] Abou-zeid, M. Y., Effects of thermal-diffusion and viscous dissipation on peristaltic flow of micropolar non-Newtonian nanofluid: application of homotopy perturbation method. *Results Phys.***6**, 481–495 (2016).

[27] Mohamed M. A. & Abou-zeid, M. Y., Peristaltic flow of micropolar Casson nanofluid through a porous medium between two co-axial tubes. *J. Porous Media***22**(9), 1079–1093 (2019).

[28] Mansour H. M. & Abou-zeid, M. Y., Heat and mass transfer effect on non-Newtonian fluid flow in a non-uniform vertical tube with peristalsis. *J. Adv. Res. Fluid Mech. Therm. Sci.***61**(1), 44–62 (2019).

[29] Eldabe, N. T., Hassan, M. A. & Abou-zeid, M. Y., Wall properties effect on the peristaltic motion of a coupled stress fluid with heat and mass transfer through a porous media. *J. Eng. Mech.***142**(3), 04015102 (2016).

[30] Eldabe, N. T. M., Rizkallah, R. R., Abou-zeid, M. Y. &Ayad, V. M., Thermal diffusion and diffusion thermo effects of Eyring-Powell nanofluid flow with gyrotactic microorganisms through the boundary layer, *Heat Transf.–Asian Res.***49**, 383 – 405 (2020).

[31] Ouaf, M. E. & Abou-zeid, M., Electromagnetic and non-Darcian effects on a micropolar non-Newtonian fluid boundary-layer flow with heat and mass transfer. *Int. J. Appl. Electromagn. Mech.***66**, 693-703 (2021).

[32] Eldabe, N. T., and Abouzeid, M. Y. &Ali, H. A., Effect of heat and mass transfer on Casson fluid flow between two co-axial tubes with peristalsis,*J. Adv. Res. Fluid Mech. Therm. Sci.***76**, 54–75 (2020).

[33] Eldabe, N. T., Moatimid, G. M., Abouzeid, M. Y., ElShekhipy, A. A., & Abdallah, N. F., A semianalytical technique for MHD peristalsis of pseudoplastic nanofluid with temperature-dependent viscosity: Application in drug delivery system. *Heat Transf.–Asian Res.***49**(1) 424–440 (2020).

[34] Eldabe, N. T. & Abou-zeid, M. Y., Radially varying magnetic field effect on peristaltic motion with heat and mass transfer of a non-Newtonian fluid between two co-axial tubes. *Therm. Sci.***22**, 2449–2458 (2018).

[35] Abou-zeid, M. Y., Homotopy perturbation method to gliding motion of bacteria on a layer of power-law nanoslime with heat transfer. *J. Comput. Theor. Nanosci.***12**, 3605–3614 (2015).

[36] Eldabe, N. T., Abou-zeid, M. Y., El-Kalaawy, O. H., Moawad, S. M. & Ahmed, O.S., Electromagnetic steady motion of Casson fluid with heat and mass transfer through porous medium past a shrinking surface. *Therm. Sci.***25**, 257–265 (2021).

[37] Eldabe, N. T. M., Abou-zeid, M. Y., Elshabouri, S. M., Salama, T. N. & Ismael, A. M., Ohmic and viscous dissipation effects on micropolar non-Newtonian nanofluid Al_2O_3 flow through a non-Darcy porous media. *Int. J. Appl. Electromagn. Mech.***68**, 209–221 (2022).

[38] Eldabe, N. T. M., Moatimid, G. M., Abou-zeid,

M., Elshekhipy, A. A. & Abdallah, N. F., Semi-analytical treatment of Hall current effect on peristaltic flow of Jeffery nanofluid. *Int. J. Appl. Electromagn. Mech.***7**, 47–66 (2021).

[39] Eldabe, N. T., Abou-zeid, M. Y., Mohamed, M. A. & Abd-Elmoneim, M. M., Peristaltic flow of Herschel Bulkley nanofluid through a non-Darcy porous medium with heat transfer under slip condition. *Int. J. Appl. Electromagn. Mech.***66**, 649–668 (2021).

[40] Abou-zeid, M. Y., Magnetohydrodynamic boundary layer heat transfer to a stretching sheet including viscous dissipation and internal heat generation in a porous medium. *J. Porous Media***14**, 1007–1018 (2011).

[41] Eldabe, N. T. M., Abou-zeid, M. Y., Ouaf, M. E., Mustafa D. R. & Mohammed, Y. M., Cattaneo–Christov heat flux effect on MHD peristaltic transport of Bingham Al_2O_3 nanofluid through a non – Darcy porous medium. *Int. J. Appl. Electromagn. Mech.***68**, 59–84 (2022).

[42] Eldabe, N. T., Elshabouri, S., Elarabawy, H., Abouzeid, M. Y. & Abuiyada, A., Wall properties and Joule heating effects on MHD peristaltic transport of Bingham non-Newtonian nanofluid. *Int. J. Appl. Electromagn. Mech.***69**(1), 87–106 (2022).

[43] Ouaf, M. E. & Abou-zeid, M. Y., Hall currents effect on squeezing flow of non-Newtonian nanofluid through a porous medium between two parallel plates. *Case Stud. Therm. Eng.***28**, 10362 (2021).

[44] Mohamed, Y. M., Eldabe, N. T., Abou-zeid, M. Y., Oauf, M. E.& Mostapha, D. R., Effects of thermal diffusion and diffusion thermo on a chemically reacting MHD peristaltic transport of Bingham plasticnanofluid.*J. Adv. Res. Fluid Mech. Therm. Sci.***98** (1), 1-17 (2022).

[45] Eldabe, N. T., Moatimid, G. M., Abou-zeid, M. Y., Elshekhipy, A. A. & Abdallah, N. F., Instantaneous thermal-diffusion and diffusion-thermo effects on carreau nanofluid flow over a stretching porous sheet. *J. Adv. Res. Fluid Mech. Therm. Sci.*, **72**(2), 142-157 (2020).

[46] Eldabe, N. T., Abouzeid, M. Y. & Ahmed, O. S. Motion of a thin film of a fourth grade nanofluid with heat transfer down a vertical cylinder: Homotopy perturbation method application. *J. Adv. Res. Fluid Mech. Therm. Sci.*,**66**(2), 101-113 (2020).

[47] Eldabe, N. T., Moatimid, G. M., Abou-zeid, M. Y., Elshekhipy, A. A. & Abdallah, N. F., Semi-analytical treatment of Hall current effect on peristaltic flow of Jeffery nanofluid. *Int. J. Appl. Electromagn. Mech.*, **7**(1), 47-66 (2021).

[48] Ismael, A.M., Eldabe, N.T.M., Abou-zeid, M.Y. & Elshabouri, S.M. Thermal micropolar and couple stresses effects on peristaltic flow of biviscosity nanofluid through a porous medium. *Sci. Rep.*, 12, 16180 (2022).

[49] Abou-zeid, M. Y., Chemical reaction and non-Darcian effects on MHD generalized Newtonian nanofluid motion, *Egypt. J. Chem*., **65**(12), 647-655 (2022).

[**50**] Shaaban, A.A., Abou-Zeid, M.Y. Effects of heat and mass transfer on MHD peristaltic flow of a non-newtonian fluid through a porous medium between two co-axial cylinders, Mathematical Problems in Engineering, 819683 (2013).

[**51**] Eldabe, N.T., Abou-Zeid, M.Y. The wall properties effect on peristaltic transport of micropolar non-newtonian fluid with heatand mass transfer, MathematicalProblems in Engineering, 808062 (2010).

[**52**]Eldabe, N. T., Abouzeid, M. Y. Mohamed, M. A. A., Abd-Elmoneim, M. M. Peristaltic mixed convection slip flow of a Bingham nanofluid through a non-darcy porous medium in an inclined non-uniform duct with viscous dissipation and radiation. J. Appl. Nonlinear Dyn. 12, 231-243 (2023).

[**53**]Abou-zeid, M. Y. Homotopy perturbation method to MHD non-Newtonian nanofluid flow through a porous medium in eccentric annuli with peristalsis Therm. Sci. 21, 2069-2080 (2015).

[**54**] Abuiyada, A. Eldabe, N. T., Abouzeid, M. Y. Elshabouri, S. Influence of both Ohmic dissipation and activation energy on peristaltic transport of Jeffery nanofluid through a porous media, CFD Letters 15, Issue 6 (2023) 65-85.